

OPTICAL CLOCKS BASED ON ULTRACOLD NEUTRAL STRONTIUM ATOMS

M. BOYD, A. LUDLOW, T. ZELEVINSKY, S. FOREMAN, S. BLATT, M. NOTCUTT, T. IDO, AND J. YE
*JILA, National Institute of Standards and Technology, and the Department of Physics, University of Colorado, 440
UCB Boulder, CO 80309-0440, U.S.A.*

I. INTRODUCTION

Ultra-cold alkaline earth atoms show great promise as future optical frequency standards and as key components in optical atomic clocks. Atomic strontium is an exciting candidate for a future standard as the level structure provides multiple narrow clock transitions as well as means for efficient laser cooling to μK temperatures. A variety of measurement techniques are currently being explored for the strontium clock transitions including, free space spectroscopy of the narrow (7.5kHz) $^1\text{S}_0$ - $^3\text{P}_1$ transition in cold bosonic ^{88}Sr [1], optical lattice based spectroscopy of the sub-Hz hyperfine induced $^1\text{S}_0$ - $^3\text{P}_0$ transition in fermionic ^{87}Sr [2], and indirect spectroscopy of the strictly forbidden $^1\text{S}_0$ - $^3\text{P}_0$ transition in ^{88}Sr using an electromagnetically-induced-transparency (EIT) resonance [3, 4]. In the case of the $^1\text{S}_0$ - $^3\text{P}_0$ transitions in ^{87}Sr and ^{88}Sr , accuracies (stabilities) have been estimated to eventually reach below the 10^{-17} (10^{-18}) level.

II. LASER COOLING AND TRAPPING OF NEUTRAL STRONTIUM

As a key component of a neutral atom based optical clock, we have developed an apparatus which allows laser cooling of nearly 10^8 strontium atoms to ultracold temperatures. Reaching ultracold temperatures with large numbers of atoms (N) is essential for the development of optical atomic clocks as residual Doppler effects are reduced at lower temperatures for improved accuracy and the stability of the clock can potentially improve by \sqrt{N} . The relevant level structure for laser cooling of strontium is shown in Fig. 1(a). The strong 461nm $^1\text{S}_0$ - $^1\text{P}_1$ transition ($\sim 32\text{MHz}$) is used to create a Magneto-Optical Trap (MOT) from a Zeeman slowed beam of strontium atoms. For the most abundant isotope, ^{88}Sr ($\sim 83\%$), more than 10^8 atoms are trapped and cooled to a temperature of $\sim 2\text{mK}$. The pre-cooled atoms are then transferred to a second-stage MOT based on the narrow 689nm $^1\text{S}_0$ - $^3\text{P}_1$ transition ($\sim 7\text{kHz}$). After the second-stage MOT, 4×10^7 atoms are available for spectroscopy with temperatures below $1\mu\text{K}$. A complete description of the laser cooling apparatus as well as detailed study of narrow-line cooling dynamics for ^{88}Sr has been described elsewhere [5, 6, 7].

Our apparatus also allows laser cooling and trapping of fermionic ^{87}Sr ($\sim 7\%$ natural abundance). Unlike the bosonic isotopes of strontium ($I=0$), ^{87}Sr has a nuclear spin of $9/2$ which adds complexity to the simple level structure shown in Fig. 1(a). In the $^1\text{S}_0$ - $^1\text{P}_1$ MOT, more than 10^7 ^{87}Sr atoms can be cooled to temperatures below 1mK [8] with only minor changes to the 461nm system used for ^{88}Sr . The narrow-line cooling laser system requires a more substantial modification as the ^{87}Sr level structure requires an extra laser for optical pumping in addition to the cooling laser [9]. However, the added complexity does not prevent cooling to the ultracold regime as temperatures in the range of $2\text{-}5\mu\text{K}$ are routinely reached with more than 10^6 atoms. We have also transferred ^{88}Sr and ^{87}Sr from the intercombination MOT to an optical lattice operating at the so-called magic wavelength.

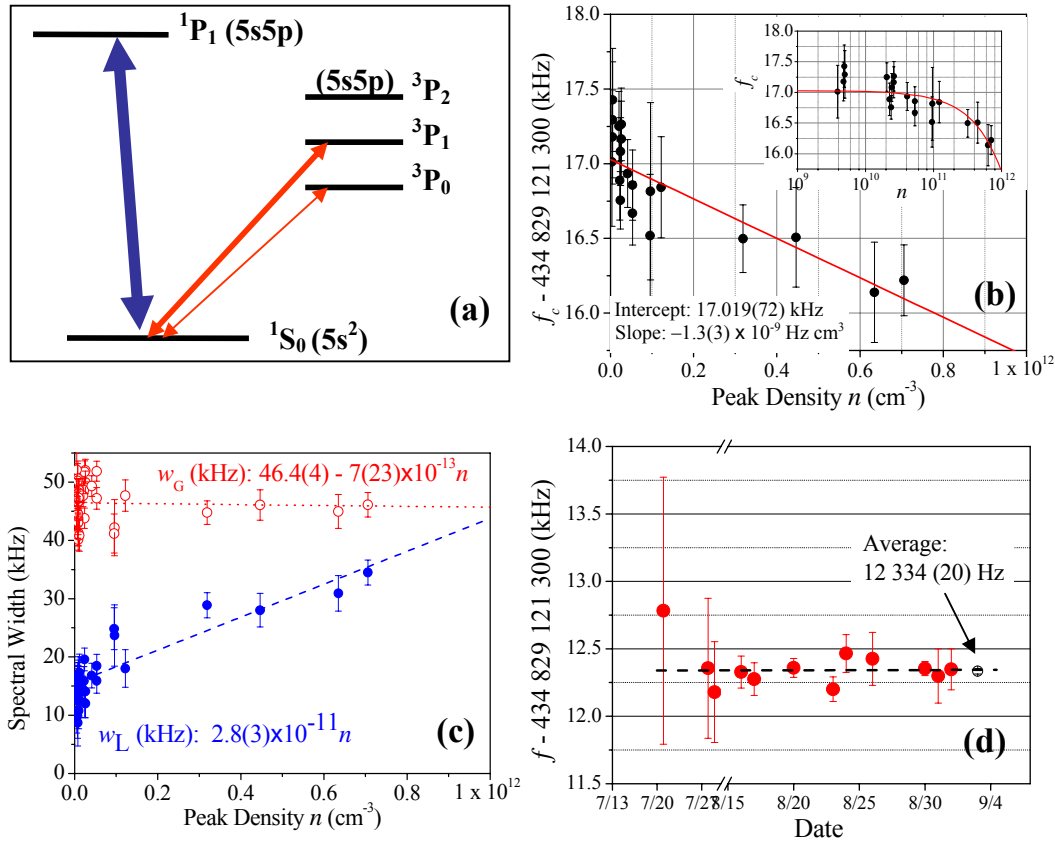


Fig. 1. (a) Relevant level structure for strontium laser cooling and spectroscopy. The strong 1S_0 - 1P_1 transition ($\lambda=461$ nm, $\Gamma=32$ MHz) is used for initial cooling and trapping. The narrow 1S_0 - 3P_1 transition ($\lambda=689$ nm, $\Gamma=7.5$ kHz) is used for second-stage cooling to μ K temperatures as well as spectroscopy. The ultra-narrow 1S_0 - 3P_0 clock transition ($\lambda=698$ nm, $\Gamma=1$ mHz), occurring only in the fermionic isotope ^{87}Sr ($I=9/2$), is also shown. (b) ^{88}Sr 1S_0 - 3P_1 transition frequency versus density over a range of three orders of magnitude. Inset shows density on a log scale. (c) Gaussian (open circles) and lorentzian (filled circles) linewidths are extracted from the voigt profiles of the spectroscopy traces in (b). While the gaussian linewidth remains constant, the lorentzian component changes significantly over the density range shown. (d) Measurement record for the 1S_0 - 3P_1 transition in ^{88}Sr , including corrections such as the photon recoil discussed in [1]. Error bars are statistical only.

III. PRECISION SPECTROSCOPY OF THE 1S_0 - 3P_1 CLOCK TRANSITION IN ^{88}Sr

The cold, dense samples of atoms produced by the laser cooling methods above provide an excellent system for spectroscopic measurement of the clock transitions in strontium. The 1S_0 - 3P_1 transition in calcium has been thoroughly explored as a frequency standard with impressive results [10] and hence the analogous ~ 7 kHz 1S_0 - 3P_1 transition in ^{88}Sr is a natural starting point for frequency metrology. Although the strontium 3P_1 lifetime is significantly shorter (a factor of ~ 20) than that of calcium, the effectiveness of the narrow line cooling in strontium results in temperature more than ten times colder than in the calcium system. This could result in higher accuracy for strontium due to a significantly reduced sensitivity to residual Doppler effects, with the caveat that the potential stability of the strontium system is lower due to the broader linewidth. With this in mind, we have performed the first precision measurement of the 1S_0 -

3P_1 clock transition using μK atoms. Using a femtosecond comb, referenced to a maser signal continuously calibrated by the NIST primary cesium standard in Boulder, we find that the absolute frequency of the 1S_0 - 3P_1 transition to be $434,829,121,312,334 \pm 20_{\text{stat}} \pm 33_{\text{sys}}$ Hz [1], shown in Fig. 1(d), which represents a 200 times improvement over previous measurements in a thermal beam [11]. To obtain this level of accuracy we have taken great care in designing our spectroscopy setup to reduce systematic shifts due to residual Doppler shifts arising from effects such as MOT drift velocities. We have also investigated the density dependence of the transition frequency (Fig. 1(b)) and linewidth (Fig. 1(c)) by varying the atom density over a range of 10^9 - 10^{12} cm^{-3} . In doing so we have observed the first definitive density related shift and broadening of a clock transition in an neutral atom alkaline-earth system, obtaining a density-related fractional frequency shift of $2.9(7) \times 10^{-24}$ cm^{-3} , which is ~ 250 times smaller than that of the cesium clock transition used to define the SI second [12]. Although the shift is relatively small, it is important to note that it exceeds a prediction based on general S-wave scattering theory and the origin of the shift needs to be explored further. For our measurement, the shift is negligible in the low density regime when compared to other systematics, such as residual Doppler effects which completely dominate the systematic error reported above, even at temperatures of $\sim 1\mu\text{K}$.

IV. SPECTROSCOPY OF THE 1S_0 - 3P_0 ^{87}Sr TRANSITION IN AN OPTICAL LATTICE

While fairly high accuracy has been achieved in measuring the 1S_0 - 3P_1 line ($\sim 8 \times 10^{-14}$), ideally one would want a narrower transition to reduce the required averaging time to reach sub-Hz ($< 10^{-15}$) accuracy, and a spectroscopic system which is free of the troublesome residual Doppler shifts. ^{87}Sr strontium offers such a transition as the hyperfine mixing of the 3P_0 , 3P_1 , and 1P_1 states provides an, otherwise completely forbidden, electric-dipole transition for 1S_0 - 3P_0 (698 nm) with an extremely narrow linewidth of $\sim 1\text{mHz}$ [13]. To measure this transition, an external cavity diode laser system at 698nm has been developed as the probe laser. This laser is stabilized to a zerodur fabry-perot cavity with a finesse of $\sim 200,000$, which is mounted in a vertical geometry to suppress the sensitivity to seismic accelerations [14]. The cavity is mounted inside a vacuum chamber, all of which rests on a commercial isolation stage for passive vibration damping. The entire laser system occupies less than 1 m^2 on the optical table. To measure the linewidth of the probe laser, an octave spanning fs-comb [15] is used to link the optical frequencies of the probe laser and a sub-Hz Nd:YAG reference laser [14] at 1064 nm. The carrier-envelope offset frequency is stabilized via a self-referencing technique [16] while the repetition frequency of the comb is stabilized by phase locking one of the comb components to the 698nm laser. A beat is then measured between the reference laser and a corresponding comb mode at 1064nm. The FWHM of the effective beat, shown in Fig. 2, is ~ 3 Hz.

To fully exploit the $\sim\text{Hz}$ linewidth of both the probe laser and the atomic transition, it is necessary to probe the atoms for timescales of ~ 1 second. While a fountain geometry is conceivable for alkaline-earth atoms such as strontium, a very attractive alternative for increasing the interaction time was recently proposed [2] which utilizes an optical lattice operating at a wavelength where the AC stark shifts of the 1S_0 and 3P_0 clock levels are equal, allowing accurate measurement of the clock transition. One major advantage of this scheme is that the atoms can be trapped in the Lamb-Dicke regime, in which spectroscopy can be done nearly free of any recoil or Doppler shifts, similar to the case of trapped ions. Furthermore, a three dimensional lattice can be employed to eliminate collisions between atoms, and hence eliminate collision shifts. A frequency standard based on neutral atoms in an optical lattice essentially combines the best features of single trapped ions and free space neutral atoms by allowing measurement of the clock transition in Lamb-Dicke regime, while enhancing the signal to noise ratio by using one million quantum absorbers.

To implement the lattice clock with ^{87}Sr we have constructed a one-dimensional optical lattice using $\sim 500\text{mW}$ of light from a Ti:Sapphire laser tuned near the so-called magic wavelength, recently measured to be $813.420(7)$ nm [17]. More than 10^5 ^{87}Sr atoms are transferred into the lattice, which has a lifetime of ~ 1 second. The axial (radial) trap frequency of the optical lattice is $\sim 80\text{kHz}$ (500 Hz) corresponding to a Lamb-Dicke parameter of ~ 0.23 (~ 3), indicating that the atoms are (are not) in the tight confinement limit. For this trap, it is obvious then that to eliminate residual Doppler and recoil effects on the frequency measurement, the 698nm probe laser must be carefully aligned along the axis of the lattice beam to insure that only the axial motion of the atoms is observed. In the axial direction, the trap frequency is significantly larger than the both the transition linewidth and the atomic recoil frequency, hence the quantized motional states of the (nearly-)harmonic potential can be observed as is shown in Fig. 3(a). Spectroscopy of the motional sidebands is a powerful tool for studying trap dynamics as it allows measurement of the atom temperature, trap frequencies, and the band structure of the trap due to the deviation from a perfect harmonic potential.

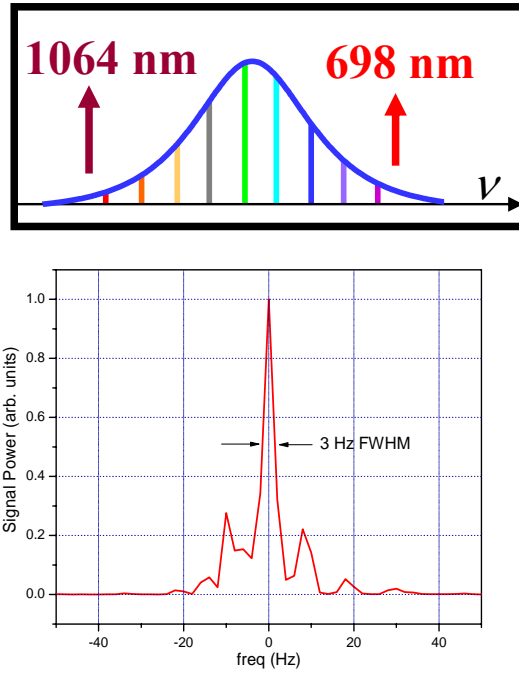


Fig. 2. Heterodyne beat between the stabilized 698nm diode laser and a sub-Hz Nd:YAG reference laser at 1064nm linked by a fs-comb.

For optical clocks, the carrier peak is most important as it is centered at the natural frequency of the atomic transition, and, the position and width of the peak are in principle independent of the lattice laser intensity when the magic wavelength is used for trapping. A typical measurement of the linewidth of the carrier is shown in Fig. 3(b) to be ~ 220 Hz. The absolute frequency of the probe laser is measured using an octave spanning fs-comb referenced, via an optical fiber link [18], to a hydrogen maser calibrated by the NIST primary cesium standard. The combination of the narrow spectrum width in Fig. 3(b) and the high stability reference frequency provided by the hydrogen maser, allowed rapid averaging of statistical uncertainties, yielding a total statistical uncertainty of 2.8 Hz for our measurement. To determine the 1S_0 - 3P_0 transition frequency with high precision and accuracy, a detailed investigation of potential systematic shifts has been performed.

The sensitivity of the clock transition to the lattice wavelength and intensity near the magic wavelength was a primary concern in terms of making a high accuracy measurement. At our typical lattice operating wavelength of 813.437(1) nm, we measured the clock transition as a function of lattice intensity, as shown in Fig 3(c), and found that at our typical operating intensity of $I_0 = 35 \text{ kW/cm}^2$, a correction of -17(8) Hz is necessary. We have also experimentally determined that, at a lattice intensity of I_0 , the sensitivity of the clock transition to the lattice wavelength deviation from λ_{magic} is $\sim 2 \text{ mHz/MHz}$. Using the measured Stark shift at 813.437nm, and the measured sensitivity to lattice wavelength deviations, we find that $\lambda_{\text{magic}} = 813.418(10)$ which is in good agreement with that reported in [17]. We have also investigated any possible density shifts by varying the number of atoms in the lattice by a factor of 50. For our typical operation density of $\sim 10^{12} \text{ cm}^{-3}$, we report a density shift of 2(13) Hz. A number of other potential shifts have been explored, including sensitivity to magnetic fields and probe intensity, allowing us to achieve a total systematic uncertainty of 20 Hz. A measurement record spanning three months is shown in Fig. 3(d) yielding a value for the ^{87}Sr 1S_0 - 3P_0 transition of $429,228,004,229,867 \pm 20_{\text{systematic}} \pm 2.8_{\text{statistical}}$ Hz. Note that the number reported disagrees at the three standard deviation level with that of [17] which was measured using a GPS uplink for the absolute frequency

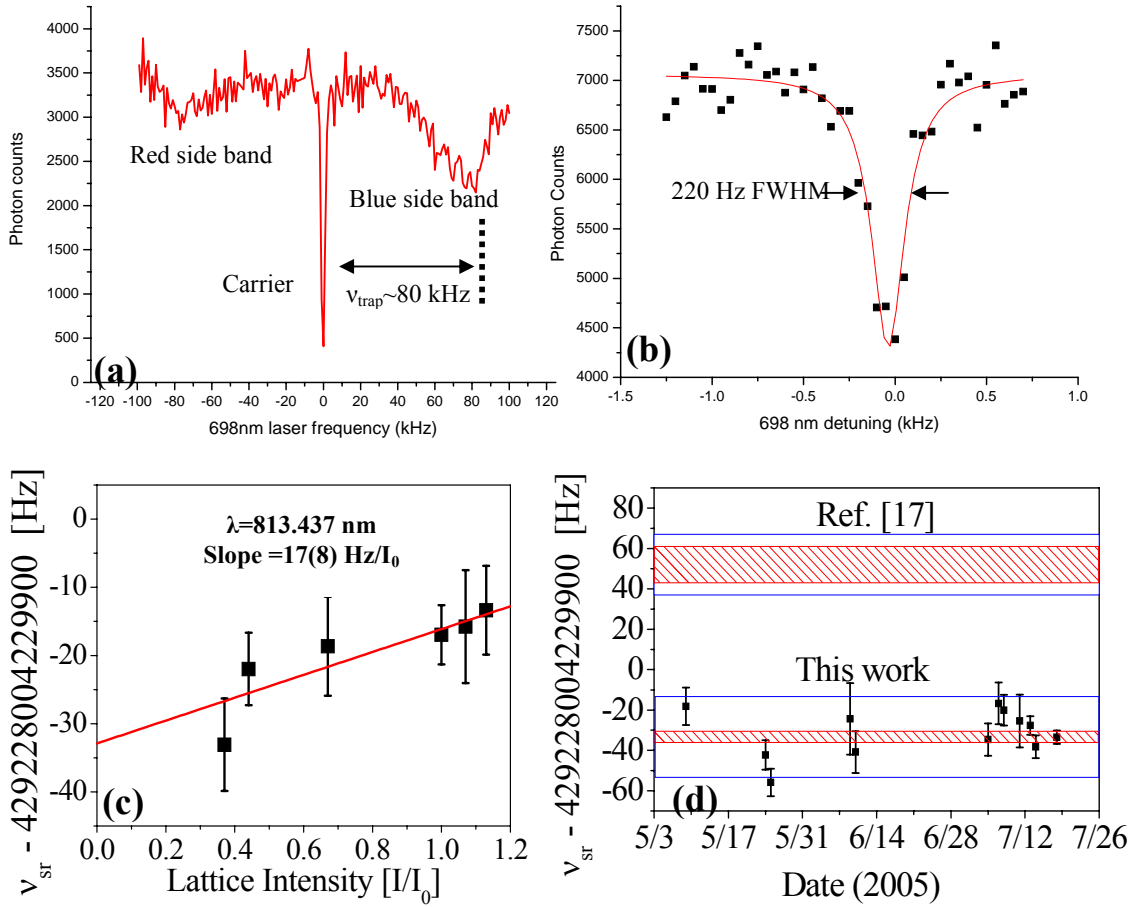


Fig. 3. (a) Spectroscopic trace over a broad range to allow observation of the motional sidebands. The red (blue) sideband represents an absorption and spontaneous emission event in which $\Delta n = -1$ ($\Delta n = +1$) where n represents the n th harmonic oscillator level in the lattice potential. The center peak, or carrier, corresponds to the clock transition shown in (b) and is due to transitions with $\Delta n = 0$. (c) Measurement of the clock transition as a function of lattice intensity for a lattice wavelength of 813.437 nm. I_0 ($=35 \text{ kW/cm}^2$) corresponds to the typical operating intensity of the lattice. (d) 1S_0 - 3P_0 clock transition frequency measured over a period of ~ 3 months. Each data point represents a large number of recorded spectra for the given date. The shaded area represents the statistical error (2.8 Hz) of our reported measurement. The outer box represents the total error including statistical and systematic (20 Hz) uncertainties. Comparison with the absolute frequency and uncertainties reported in [17] reveals a difference of more than three standard deviations between the JILA and Tokyo measurements.

reference. A detailed description of our ^{87}Sr lattice clock system was recently reported in [19], including narrow-line laser characterization using a fs-comb, motional sideband spectroscopy in the lattice, and the absolute frequency measurement of the clock transition. The $\sim 20 \text{ Hz}$ uncertainty (5×10^{-14} fractional uncertainty) reported here is by no means a limit to the lattice clock system. The transition linewidth can potentially be narrowed to the Hz level, allowing extremely high precision for rapid investigations of systematic shifts. Implementation of a 3-D lattice will insure tight

confinement in all three dimensions, reducing the sensitivity of the system to probe alignment. Improved measurements of λ_{magic} should allow operation of the lattice clock with sub-Hz accuracy in terms of the lattice Stark shift. While the potential of the ^{87}Sr lattice clock is impressive, it is essential that the discrepancy between reported values be resolved.

V. AN ENGINEERED CLOCK TRANSITION IN BOSONIC STRONTIUM USING EIT

While ^{87}Sr offers an extremely exciting and promising optical clock transition, the hyperfine sublevels (m_f) may limit the eventual accuracy of such a system as a linear Zeeman shift of $\sim 100 \times m_f \text{ Hz/Gauss}$ exists due to the difference in the ground and excited state g -factors [20]. The sublevels also have a weak sensitivity to the lattice polarization which could be an eventual limitation [2]. The Zeeman shift may hinder the stability of the system as well if multiple sub-levels need to be scanned before the true line center is known. The ultimate stability of the system may also be limited by the low natural abundance (7%) and longer cooling times required for narrow-line cooling in the presence of hyperfine structure. With this in mind, it seems that the 1S_0 and 3P_0 energy levels in ^{88}Sr are better suited for a lattice based standard for a variety of reasons. (i) The accuracy of the standard should be improved since the linear Zeeman shift is non-existent, and the clock states are completely scalar, eliminating sensitivity to the lattice polarization, (ii) the

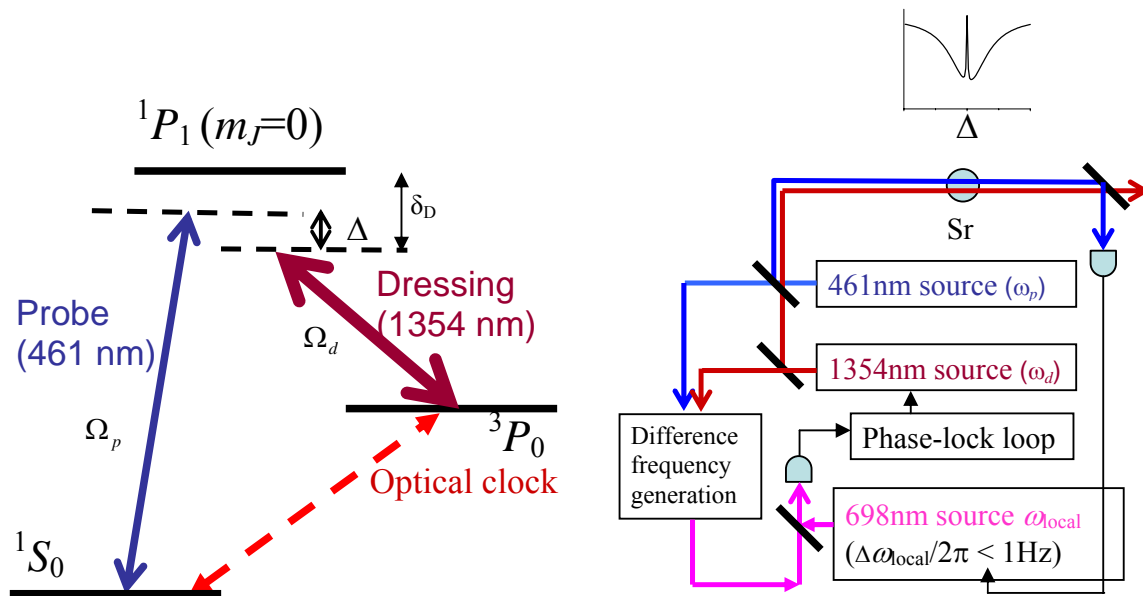


Fig. 4. Three level EIT scheme as discussed in the text. A narrow EIT dip appears in the broad 1S_0 - 1P_1 transition spectrum when the difference between the probe and dressing laser frequencies equals the frequency separating the 1S_0 and 3P_0 clock states. In this case, the optical clock frequency is not directly measured, but instead is generated by using a Difference Frequency Generation (DFG) system to procure the clock frequency. The generated clock light can then be stabilized to a local oscillator at 698 nm, such as the one described in section IV of the text, by feeding back to the dressing or probe laser. The EIT signal completes the feedback loop by steering the local oscillator.

large natural abundance (83%) and simple hyperfine-free level structure of ^{88}Sr would give an improved stability by improving the signal to noise ratio, and (iii) the laser cooling setup is less complex and more efficient. While ^{88}Sr seems the ideal candidate, one problem lingers, the $^1\text{S}_0$ - $^3\text{P}_0$ transition is completely forbidden in the absence of hyperfine structure. However, the potential benefits of pursuing this standard in ^{88}Sr have motivated a new experiment using an Electromagnetically Induced Transparency (EIT) resonance to indirectly measure the strictly forbidden $^1\text{S}_0$ - $^3\text{P}_0$ transition [3]. The basic strategy of the EIT based optical clock is shown in Fig 4.

A dressing laser at 1354nm and a probe laser at 461nm are used to coherently couple the $^1\text{S}_0$ and $^3\text{P}_0$ clock states through the short-lived $^1\text{P}_1$ state. When the difference of the frequencies of the probe and dressing lasers is equal to the energy difference of the two clock states (i.e. $\Delta=0$), an extremely narrow EIT dip emerges in the broad $^1\text{P}_1$ absorption profile. Since the EIT dip depends only on the difference frequency of the two lasers, the relative detuning of the dressing and probe lasers from the $^1\text{P}_1$ state does not affect the measured $^1\text{S}_0$ - $^3\text{P}_0$ frequency. The width of the EIT dip is determined from the Rabi frequency of the dressing laser, Ω_d , the linewidth of the $^1\text{P}_1$ state, γ , and the relative detuning of the dressing laser from the $^1\text{P}_1$ state, δ_D . The linewidth is given by:

$$\gamma_{\text{EIT}} = \frac{\Omega_d^2}{\gamma} \left\{ 1 - 8[\delta_D / \gamma]^4 + \mathcal{O}([\delta_D / \gamma]^6) \right\} \quad (1)$$

Equation (1) clearly shows that the EIT clock can operate at a variable linewidth simply by changing the intensity of the dressing laser. It is also evident that the line-shape of the EIT dip also depends very weakly on the detuning of the dressing laser, when the detuning is small compared to the large natural linewidth of the $^1\text{P}_1$ state (32 MHz). Since the position of the $^1\text{P}_1$ state does not affect the position or lineshape of the EIT dip, this system should work equally well in a magic wavelength lattice. Although the lattice will shift the $^1\text{P}_1$ state (the lattice is only ‘magic’ for the clock states), for the lattice parameters discussed above the shifts will be in the hundreds of kHz range, which is still quite small compare to the $^1\text{P}_1$ linewidth. One concern for the EIT scheme is the AC stark shifts of the clock levels due to the probe and dressing lasers. The AC stark shift for a probe laser intensity of $\sim 10\mu\text{W}/\text{cm}^2$ is estimated to be below 1 mHz. For the dressing laser, an intensity of $\sim 3.9\text{mW}/\text{cm}^2$ is required to broaden the EIT dip 1 mHz, an equivalent linewidth to that provided by nature in ^{87}Sr . At this intensity, the stark shift due to the dressing laser is estimated to be -21mHz. This scheme has been estimated to eventually achieve an accuracy of $< 2 \times 10^{-17}$. Practical implementation of this system seems reasonable, as the probe and dressing laser do not need to be individually stabilized to a high precision (due to the insensitivity to the $^1\text{P}_1$ detuning); only the difference frequency needs to be precisely stabilized. One implementation scheme is shown in Fig. 4, in which the difference frequency of the probe and dressing lasers is phase locked to a highly stabilized clock laser at 698nm. The lock only provides feedback to the dressing laser, ensuring that any fluctuations in the probe laser will be followed by the dressing laser in order to keep the difference frequency stable at the 1 Hz level. The EIT dip can then be scanned by tuning the 698 clock laser, and the clock laser can finally be stabilized to the strontium atoms by locking to the EIT peak. It should be noted that the EIT scheme could potentially be used for atoms with similar level structure such as Mg, Ca, Yb, and Hg, depending on the severity of the stark shifts from the probe and dressing lasers.

VI. CONCLUSION

In summary, we have developed an apparatus which allows laser cooling and trapping of $>10^7$ bosonic ^{88}Sr ($\sim 10^6$ fermionic ^{87}Sr) atoms to temperature below $1\mu\text{K}$ ($\sim 2\text{-}5\mu\text{K}$). Using these cold dense samples we have performed high accuracy frequency metrology on the $^1\text{S}_0$ - $^3\text{P}_1$ transition in ^{88}Sr yielding a value of $434,829,121,312,334 \pm 20_{\text{stat}} \pm 33_{\text{sys}}$ Hz, which was completely limited by Doppler effects. We observed a definitive density-related shift of the clock transition for the first time in an alkaline-earth atom system. A highly stabilized diode laser ($<5\text{Hz}$) has been developed for spectroscopy of the ultra-narrow $^1\text{S}_0$ - $^3\text{P}_0$ clock transition in ^{87}Sr . Using this laser system we have observed motional sidebands of atoms trapped in an optical lattice which operates at a wavelength such that the net Stark shift is zero. The linewidth of the observed clock transition has been reduced to the 200 Hz level. Absolute frequency metrology of the transition has been performed, including a systematic study of potential frequency shifts, using an octave-spanning fs-

comb to provide the phase-coherent link between the strontium clock and the NIST primary cesium standard referenced hydrogen maser. We report a value for the $^{87}\text{Sr } ^1\text{S}_0\text{-}^3\text{P}_0$ clock transition of $429,228,004,229,867 \pm 20_{\text{sys}} \pm 2.8_{\text{stat}}$ Hz. Finally, we have presented a novel clock scheme using EIT to indirectly probe the strictly forbidden $^1\text{S}_0\text{-}^3\text{P}_0$ transition in ^{88}Sr . The linewidth of the EIT dip can be easily varied, and the AC stark shifts can be controlled to achieve an estimated accuracy of $< 2 \times 10^{-17}$. The EIT scheme may prove to produce a more accurate and stable clock than the natural clock transition in ^{87}Sr due to the complete insensitivity of the clock transition to lattice polarization and first order Zeeman shifts.

VII. ACKNOWLEDGEMENTS

We gratefully acknowledge the contributions of T. Loftus on the laser cooling and trapping apparatus and precision spectroscopy of the $^1\text{S}_0\text{-}^3\text{P}_1$ transition, J. Hall and L.S. Ma on the development of narrow linewidth lasers, and R. Santra, E. Arimondo, and C. Greene on development of the EIT-based clock proposal. Funding is provided by ONR, NSF, NASA, and NIST.

VIII. REFERENCES

- [1] T. Ido, T. Loftus, M. M. Boyd, A. D. Ludlow, K. W. Holman, and J. Ye, *Phys. Rev. Lett.*, **94**, 153001 (2005).
- [2] H. Katori, M. Takamoto, V. G. Pal'chikov, and V. D. Ovsianikov, *Phys. Rev. Lett.* **91**, 173005 (2003).
Masao Takamoto and Hidetoshi Katori, *Phys. Rev. Lett.* **91**, 223001 (2003)
- [3] R. Santra, T. Ido., E. Arimondo, C. H. Greene, and J. Ye, *Phys. Rev. Lett.* **94**, 173002 (2005).
- [4] T. Hong, C. Cramer, W. Nagourney, and E. N. Fortson, *Phys. Rev. Lett.* **94**, 050801 (2005).
- [5] T. Loftus, T. Ido, M. M. Boyd, A. D. Ludlow, and J. Ye, *Phys. Rev. A* **70**, 063414 (2004).
- [6] T. Loftus, T. Ido, A. D. Ludlow, M. M. Boyd, and J. Ye, *Phys. Rev. Lett.* **93**, 073003 (2004).
- [7] H. Katori, T. Ido, Y. Isoya, and M. Kuwata-Gonokami, *Phys. Rev. Lett.* **82**, 1116 (1999).
- [8] X. Xu, T. Loftus, J. W. Dunn, C. H. Greene, J. L. Hall, A. Gallagher, and J. Ye, *Phys. Rev. Lett.* **90**, 193002 (2003).
- [9] T. Mukaiyama, H. Katori, T. Ido, Y. Li, and M. Kuwata-Gonokami, *Phys. Rev. Lett.* **90**, 113002 (2003).
- [10] See for example Th. Udem, S. A. Diddams, K. R. Vogel, C. W. Oates, E. A. Curtis, W. D. Lee, W. M. Itano, R. E. Drullinger, J. C. Bergquist, and L. Hollberg, *Phys. Rev. Lett.* **86**, 4996 (2001).
G. Wilpers, T. Binnewies, C. Degenhardt, U. Sterr, J. Helmcke, and F. Riehle, *Phys. Rev. Lett.* **89**, 230801 (2002).
And the two proceedings presented at this conference by C. W. Oates, and U. Sterr.
- [11] G. Ferrari, P. Cancio, R. Drullinger, G. Giusfredi, N. Poli, M. Prevedelli, C. Toninelli, and G. Tino, *Phys. Rev. Lett.* **91**, 243002 (2003).
I. Courtillot, A. Quessada-Vial, A. Brusch, D. Kolker, G. D. Rovera, and P. Lemonde, physics/0410108.
- [12] Y. Sortais, S. Bize, C. Nicolas, G. Santarelli, G. S. C. Salomon, and A. Clairon, *IEEE Trans. Ultrason. Ferroelectr. Freq. Control* **47**, 1093 (2004).
- [13] V. G. Pal'chikov, *Proc. Of EFTF-2002*, St. Petersburg, (2002).
Sergey G. Porsev and Andrei Derevianko, *Phys. Rev. A* **69**, 042506 (2004).
- [14] M. Notcutt, L.-S. Ma, J. Ye, and J. L. Hall, *Optics Letters*, in press.
- [15] T. M. Fortier, D. J. Jones, and S. T. Cundiff, *Optics Letters*, **28**, No. 22 (2003).
- [16] D. J. Jones, S. A. Diddams, J. K. Ranka, A. Stentz, R. S. Windeler, J. L. Hall, and S. T. Cundiff, *Science* **288**, 635 (2000).
- [17] M. Takamoto, F.-L. Hong, R. Higashi, and H. Katori, *Nature* **435**, 321 (2005).
- [18] J. Ye,
- [19] A. D. Ludlow, M. M. Boyd, T. Zelevinsky, S. Foreman, S. Blatt, M. Notcutt, T. Ido, and J. Ye, *arXiv:physics/0508041*.
- [20] E. Peik, G. Hollemann, and H. Walther, *Phys. Rev. A* **49**, 402 (1994).